Validation and use of a musculoskeletal gait model to study the role of functional electrical stimulation

Ding, Ziyun; Azmi, Nur Liyana; Bull, Anthony

Validation and Use of a Musculoskeletal Gait Model to Study the Role of Functional Electrical Stimulation

Ziyun Ding [ID], Nur Liyana Azmi [ID], and Anthony M. J. Bull [ID]

Abstract—Objective: Musculoskeletal modeling has been used to predict the effect of functional electrical stimulation (FES) on the mechanics of the musculoskeletal system. However, validation of the resulting muscle activations due to FES is challenging as conventional electromyography (EMG) recording of signals from the stimulated muscle is affected by stimulation artefacts. A validation approach using a combination of musculoskeletal modeling and EMG was proposed, whereby the effect on nonstimulated muscles is assessed using both techniques. The aim is to quantify the effect of FES on biceps femoris long head (BFLH) and validate this directly against EMG of gluteus maximus (GMAX). The hypotheses are that GMAX activation correlates with BFLH activation; and the muscle activation during FES gait can be predicted using musculoskeletal modeling. *Methods*: Kinematics, kinetics, and EMG of healthy subjects were measured under four walking conditions (normal walking followed by FES walking with three levels of BFLH stimulation). Measured kinematics and kinetics served as inputs to the musculoskeletal model. *Results*: Strong positive correlations were found between GMAX activation and BFLH activation in early stance peak ($R = 0.78$, $p = 0.002$) and impulse ($R = 0.63$, $p = 0.021$). The modeled peak and impulse of GMAX activation increased with EMG peak ($p < 0.001$) and impulse ($p = 0.021$). *Conclusion*: Musculoskeletal modeling can be used reliably to quantify the effect of FES in a healthy gait. *Significance*: The validation approach using EMG and musculoskeletal modeling developed and tested can potentially be applied to the use of FES for other muscles and activities.

Index Terms—Functional electrical stimulation, musculoskeletal modelling.

I. INTRODUCTION

FUNCTIONAL electrical stimulation (FES) involves utilising patterned electrical stimulation to nervous tissue in order to activate muscles [1]. The beneficial effects of FES have been demonstrated for individuals with neurological pathologies [2]–[5]. Investigations have been made to artificially elicit and control lower limb muscle contraction via FES thereby utilising the musculature and metabolic power supply of individuals to generate locomotion [2], [4], [6]. In addition to the restoration of lower limb movement, FES-aided gait has also been shown to have potential benefits for individuals with orthopaedic pathologies, including mitigation of medial knee loading for patients with knee osteoarthritis (OA) [7], [8], and improvement in knee stability for patients with anterior cruciate ligament (ACL) injuries [9], [10].

In order to control graded force recruitment from selective muscles and produce well-coordinated movement via FES, the knowledge of muscle activations in magnitude and timing is important. Advances in computational musculoskeletal gait models provide promising, non-invasive determination of mechanical loading in a musculoskeletal system. Such models take as input measured kinematics (joint angles and segment positions) and kinetics (ground reaction force and segmental parameters) during gait to formulate the equations of motion; solving these yields muscle, joint and ligament forces. However, validating the results from the musculoskeletal models is a well-known challenge [11]–[13]. Validation can be achieved at the level of tendon forces, bone forces or joint contact forces using invasive devices, for example instrumented prostheses [14], [15] or tendon transducers [16]. Alternatively, validation is possible at the level of muscle activations with surface electromyography (EMG) [17], [18].

EMG signals are affected by the stimulation artefacts caused by the stimulation current when FES is used. This has been partially addressed in the literature with, for example, use of an EMG-amplifier with shut-down control [19], advanced filtering procedures [19]–[21], and optimising the positioning of the EMG electrodes in relation to the stimulation electrodes [20], [22]. These approaches do not fully eliminate the stimulation artefacts.

Due to the difficulties in detecting EMG signals from the same electrically stimulated muscle, the approach proposed in this study is to measure EMG signals from a non-stimulated

muscle that is sufficiently far removed from the stimulator. The muscle must also have the feature that it is likely to change its activation due to the disrupted mechanics produced by the stimulated muscle's increased activation. It is therefore necessary to identify such a pair of muscles, where the activation of one is likely to have an effect on the activation of the second muscle. Biceps femoris long head (BFLH) and gluteus maximus (GMAX) is a pair of the muscle candidates. BFLH acts as a knee flexor, and potentially compensates for weak hip extensors such as GMAX [23]. Clinically, stimulation of BFLH via FES has been used to generate hip extension for patients with paraplegia [6], and improve knee stability for patients with ACL deficiency [24]. Therefore, BFLH is a clinically useful muscle in FES assisted gait. The aim of this study is to quantify the effect of FES on BFLH during gait utilising a musculoskeletal model and validate this directly against EMG of GMAX. The hypotheses of the study are that: GMAX activation correlates with BFLH activation; and the muscle activation pattern during FES gait with stimulation of BFLH can be predicted from the computational MSK model.

II. METHODS AND MATERIALS

The hypotheses were tested through computational modelling, three-dimensional gait analysis of healthy subjects under four walking conditions (normal walking followed by FES walking implemented in three output current amplitudes on BFLH), and the simultaneous measurement of EMG of GMAX. Thirteen healthy subjects (5 males and 8 females; mean height 1.65 ± 0.12 m; mass 64 ± 13 kg; age 26 ± 3 years) participated in the study. This study was approved by the institutional research ethics committee of Imperial College London and written informed consent was obtained from all participants.

A. Data Collection

Kinematic and kinetic data were collected in the motion laboratory, Department of Bioengineering, Imperial College London, UK. Eighteen retro-reflective markers were placed on the pelvis and the right lower limb (see Fig. 1) [10]. Their trajectories were captured at 200 Hz using a ten-camera motion capture system (VICON, Oxford Metrics Group, UK). Ground reaction forces of the right limb were recorded at 2000 Hz from a force plate (Kistler, Kistler Instrument AG, Switzerland). Initially, subjects performed six normal walking trials along an approximately six-metre level walkway at a self-selective comfortable walking speed, taking several steps prior to landing the right foot entirely on the force plate, and continuing for several steps. Following the normal walking trials, the skin of BFLH region was cleaned with a 70% isopropyl alcohol wipe and allowed to dry in seconds. Two rubber and gel electrodes (7 cm in diameter, PALS, Axelgaard manufacturing co., ltd, USA) were placed in the region: one in the centre between the ischial tuberosity to the lateral femoral epicondyle and the other one approximately 10 cm distally to the first (Fig. 1). Electrical stimuli were delivered via the electrodes from a two-channel stimulator (O2CHS II, Odstock Medical Limited, UK), set at 40 Hz frequency with a pulse width of approximately 120 μs; this setting
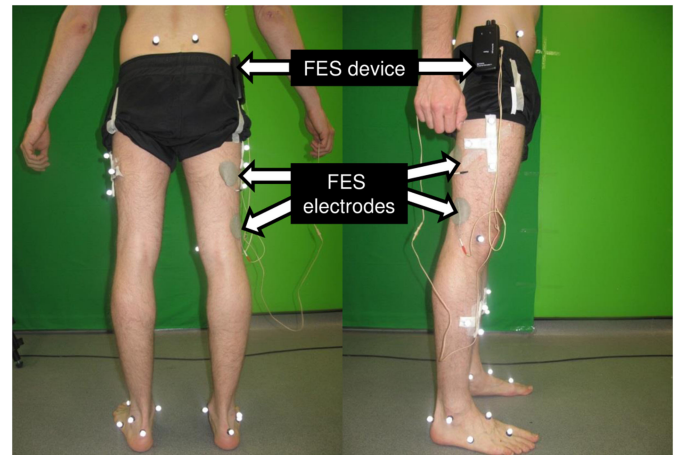

Fig. 1. Optical motion tracking markers and FES electrodes positioning.

was tolerated by the majority of subjects in our previous study [10]. The output current amplitude was set to three stimulation levels of 40 mA, 60 mA and 80 mA. Six walking trials were measured for each stimulation level. To test that the BFLH stimulation was consistently applied between subjects, prior to FES gait, subjects were asked to stand with their legs straight and the stimulator was activated. The electrode positions and stimulation level were confirmed when a clear contraction of BFLH was observed through the resulting flexion of the right knee.

Surface EMG (Delsys, Trigno Wireless EMG System, USA) was sampled at 2000 Hz for BFLH and GMAX of the right limb. According to the SENIAM recommendations [25] sensors were placed at halfway along the line between the ischial tuberosity and the lateral femoral epicondyle for BFLH; and halfway along the line between the sacral vertebrae and the greater trochanter for GMAX. Prior to sensor placement, the skin area was shaved and cleaned with alcohol wipe to reduce skin impedance and to ensure electrode adhesion. During FES walking trials, the sensor at the region of BFLH was replaced with the FES electrodes. EMG was corrected for offset, high-pass filtered at 30 Hz using a zero phase-lag, four order Butterworth filter and rectified. The rectified signals were then low-pass filtered at 10 Hz [26].

B. Lower Limb Musculoskeletal Model

An open source musculoskeletal modelling software Freebody was used (V2.1, [27], [28]). The segment-based lower limb model consists of the foot, shank, thigh, pelvis and patella segments. The model inputs are the kinematics data from the retro reflective markers and the kinetics data from the force plate. In terms of the inverse dynamics method, the model calculates the intersegmental forces and moments at the proximal end of each segment [29].

Freebody's musculoskeletal dataset consists of 163 muscle elements representing 38 lower limb muscles. The muscle attachment sites, joint centres of rotation, and tibiofemoral contact points were manually digitized from the MR imaging of a male subject (1.83 m, 96.0 kg, 44.0 years) [27]. The model estimates the muscular and joint reaction forces experienced by the lower

limb during the recorded movement. The optimisation was performed using the cost function in order to minimise the sum of the cubed muscle activations [30] as:

$$Min \sum_{i=1}^{163} \left(\frac{f_i}{f_{max_i}} \right)^3 \quad (1)$$

where f_i is the muscle force of muscle element i ($i = 1, \ldots, 163$) and f_{max_i} is the maximum muscle force of muscle element i, which is determined by multiplying published physiological cross-sectional areas of muscle element i by an assumed maximum muscle stress of 31.39 N/cm^2 [31], constrained by the equations of motion of the whole lower limb as:

$$\begin{bmatrix} S_i \\ M_i \end{bmatrix} = \begin{bmatrix} m_i E_{3\times3} & 0_{3\times3} \\ m_i c_i & I_i \end{bmatrix} \begin{bmatrix} a_i - g \\ \ddot{\theta}_i \end{bmatrix}$$
$$+ \begin{bmatrix} 0_{3\times1} \\ \dot{\theta}_i \times I_i \dot{\theta}_i \end{bmatrix} \begin{bmatrix} E_{3\times3} & 0_{3\times3} \\ d_i & E_{3\times3} \end{bmatrix} \begin{bmatrix} S_{i-1} \\ M_{i-1} \end{bmatrix} \quad (2)$$

where i is the segment number or joint number (numbering from distal to proximal), S_i the proximal inter-segmental forces, S_{i-1} the distal inter-segmental forces, M_i the proximal inter-segmental moments (notional joint moments), M_{i-1} the distal inter-segmental moments (notional joint moments), I_i the inertia tensor, $\ddot{\theta}_i$ the angular acceleration about COM, $\dot{\theta}_i$ the angular velocity about the COM, a_i the linear acceleration of COM, m_i the segment mass, E_{3X3} the identity matrix, c_i the vector from the proximal joint to the segment COM and d_i is the vector from the proximal to the distal joint.

C. Revised Optimisation Method

In order to simulate the effect of three FES current levels applied to BFLH, a modified optimisation method was used [10]. In this method the muscle force of BFLH is set as a constant value during the stance phase which is equal to the muscle activation, c, times the maximum force of BFLH. As the attachment sites of BFLH are on the shank and thigh segments, the equations of motion of the shank and thigh segments were modified by the inclusion of an additional term to give:

$$\begin{bmatrix} S_i \\ M_i \end{bmatrix} = \begin{bmatrix} m_i E_{3\times3} & 0_{3\times3} \\ m_i c_i & I_i \end{bmatrix} \begin{bmatrix} a_i - g \\ \ddot{\theta}_i \end{bmatrix} + \begin{bmatrix} 0_{3\times1} \\ \dot{\theta}_i \times I_i \dot{\theta}_i \end{bmatrix}$$
$$+ \begin{bmatrix} E_{3\times3} & 0_{3\times3} \\ d_i & E_{3\times3} \end{bmatrix} \begin{bmatrix} S_{i-1} \\ M_{i-1} \end{bmatrix}$$
$$- \begin{bmatrix} (c \times f_{BFLH_{max}}) \cdot n_{BFLH} \\ (c \times f_{BFLH_{max}}) \cdot (r_{BFLH} \times n_{BFLH}) \end{bmatrix} \quad (3)$$

where c is a constant, $f_{BFLH max}$ the maximum force of BFLH, n_{BFLH} the line of action of BFLH and r_{BFLH} the moment arm of BFLH. The muscle forces of the remaining 162 muscles were re-optimised based on the modified equations of motion. From our previous study, a mean BFLH activation value of 0.208 reduces the peak anterior shear force below zero [10] which is the maximum desired clinical outcome for those with ACL

deficiency. In this study, c was set to 0.10, 0.15 and 0.20; these are all greater than the BFLH activation predicted from normal optimisation and not greater than the maximum value required from the previous study. Measured kinematics and kinetics during normal walking and walking with FES currents of 40 mA, 60 mA and 80 mA were set as inputs for the normal optimisation as well as for revised optimisation with c values of 0.10, 0.15 and 0.20, respectively.

D. Data Analysis and statistics

Per subject, three random selected walking trials for each of the four conditions were processed. GMAX EMG activity was defined as the processed signals normalized by the peak value from 12 walking trials (3 walking trials × 4 conditions); this varied from 0 to 1. EMG activity and modelled activation were expressed as a percentage of the stance phase (0% is right heel strike and 100% is right heel off). Time-integrated measures (impulses) of EMG activity and modelled activation were determined using the trapezoidal method of numerical integration [32].

Statistical analysis was performed using SPSS (Version 24.0, IBM Corp., USA). Significance was set at an alpha level of 0.05. Linear regression analyses were performed to evaluate the relationship between GMAX activation and BFLH activation. Difference between conditions at walking speed, early stance peak, timing and impulse of EMG activity and modelled activation of GMAX were assessed using either one-way repeated measures ANOVA (for normally distributed variables, as inspected from the Shapiro-Wilk test) or Friedman tests (for non-normally distributed variables). Where results were significant, pairwise comparisons were performed with a Bonferroni correction for multiple comparisons. The relationship between the modelled muscle activation and EMG activity was investigated using the Restricted Maximum Likelihood (REML) linear mixed model analysis with subjects considered as the random factor. Dependent variables were the predicted GMAX early stance peak and impulse. EMG activity early stance peak and impulse were the fixed effects.

III. RESULTS

Across 13 subjects, modelled GMAX activation was plotted against the modelled BFLH activation (see Fig. 2). Strong positive correlations were found in early stance peak (R = 0.78, $p = 0.002$) and impulse (R = 0.63, $p = 0.021$).

All subjects tolerated FES output currents of 40 mA and 60 mA. One subject did not tolerate the output current of 80 mA and therefore results for FES walking with 80 mA stimulation are for 12/13 subjects.

Measured and modelled variables during stance are reported in Table I. Walking speed did not change across conditions ($p = 0.663$). GMAX EMG activity peak occurred at 13% ($\pm2\%$) of stance, the timing of which did not change across conditions ($p = 0.470$). Early stance peak and impulse of GMAX EMG activity increased significantly from normal walking to FES walking ($p < 0.001$). The musculoskeletal modelling predicted GMAX activation peak at 27% ($\pm1\%$) of stance with a lag
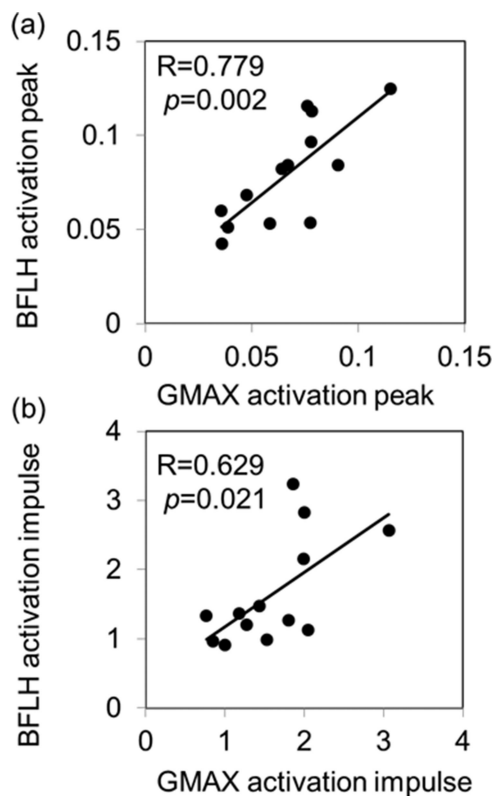
TABLE I
WALKING SPEED, MEASURED AND MODELLED VARIABLES OF GLUTEUS MAXIMUS (GMAX) DURING STANCE ACROSS CONDITIONS,
REPORTED AS MEAN (95% CI-CONFIDENCE INTERVAL)

	Normal walking (n=13)	FES walking (40mA, n=13)	FES walking (60mA, n=13)	FES walking (80mA, n=12)	p value
Speed (m/s)	1.02(0.93-1.10)	0.98(0.90-1.07)	1.00(0.91-1.08)	1.03(0.96-1.09)	0.663
Measured variables of GMAX					
Early stance peak timing (% stance)	12(8-16)	13(8-17)	11(7-15)	15(9-21)	0.470‡
Early stance EMG peak	0.52(0.47-0.58)	0.63(0.56-0.70)*	0.74(0.66-0.82)*†	0.88(0.81-0.95)*†	<0.001
Early stance EMG impulse	9.42(7.95-10.88)	11.54(9.72-13.36)*	12.90(11.00-14.81)*†	14.99(12.75-17.24)*†	<0.001
Modelled variables of GMAX					
Early stance peak timing (% stance)	25(23-27)	27(25-30)	28(25-30)	28(26-31)	0.063‡
Early stance activation peak	0.07(0.05-0.08)	0.08(0.06-0.09)*	0.09(0.08-0.11)*†	0.11(0.09-0.13)*†	0.001
Early stance activation impulse	1.32(1.09-1.55)	1.70(1.36-2.04)*	2.14(1.64-2.44)*†	2.47(1.93-3.01)*†	<0.001

*Significantly different from normal walking;
†Significantly different from FES walking with lower current;
‡ Values are from the Friedman test.

Fig. 2. Relationships between GMAX activation and BFLH activation during early stance (0–33% of stance). (a) Activation peaks and (b) activation impulses during early stance (n = 13).

TABLE II
RELATIONSHIP BETWEEN MODELLED ACTIVATION OF GLUTEUS MAXIMUS
AND EMG ACTIVITY IN EARLY STANCE PEAK AND IMPULSE

Linear mixed model	β	(95% CI)	p value
Early stance peak			
Intercept	0.0086	(-0.0163- 0.0336)	0.490
EMG peak	0.1128	(0.0777- 0.1479)	<0.001
Early stance impulse			
Intercept	1.0724	(0.3627-1.7821)	0.004
EMG impulse	0.0671	(0.0107- 0.1235)	0.021

β (95% CI): regression coefficient (95% confidence interval) estimated by the linear mixed model.

impulse (see Fig. 3(c) and (d)). Linear mixed models (see Table II) confirmed that the modelled peak and impulse of GMAX activations increased with EMG peak ($p < 0.001$) and impulse ($p = 0.021$).

IV. DISCUSSIONS

The purpose of the study was to quantify the effect of FES on BFLH using MSK modelling and validate this directly against EMG of GMAX. The first hypothesis that GMAX activation correlates with BFLH activation was confirmed through strong positive correlations between GMAX activation and BFLH activation in early stance peak (R = 0.78, $p = 0.002$) and impulse (R = 0.63, $p = 0.021$). The second hypothesis that these activations can be quantified through musculoskeletal modelling was also confirmed through validation using EMG. In the musculoskeletal model, muscle activations were calculated, constrained by the experimental measured kinematics and kinetics, and the modified BFLH activation to represent the stimulation at the output currents of 40 mA, 60 mA and 80 mA. The modelled early stance peak and impulse of GMAX activation significantly correlated with the early stance peak and impulse of EMG activity ($p \leq 0.021$). However, there was a consistent electromechanical delay of approximately 95 ms between measured EMG and modelled activation. This is comparable to other studies [33], [34]. Where others have used musculoskeletal models to quantify the effect of FES, none have validated these models against simultaneously measured EMG signals. An alternative to the method proposed here would be to use

of 14% (±2%) stance from the EMG measurement; this did not change between conditions ($p = 0.063$). Modelled early stance peak and impulse of GMAX activation increased significantly from normal walking to FES walking ($p < 0.001$).

Measured EMG activity and modelled GMAX activation is plotted in Fig. 3 for a representative subject. During early stance, the peak EMG activity was lowest for normal walking, and was positively correlated to current amplitude in FES walking. Greater c values in the optimisation models contributed to greater GMAX activation. The increase of GMAX activation peak and impulse followed the increase of EMG peak and
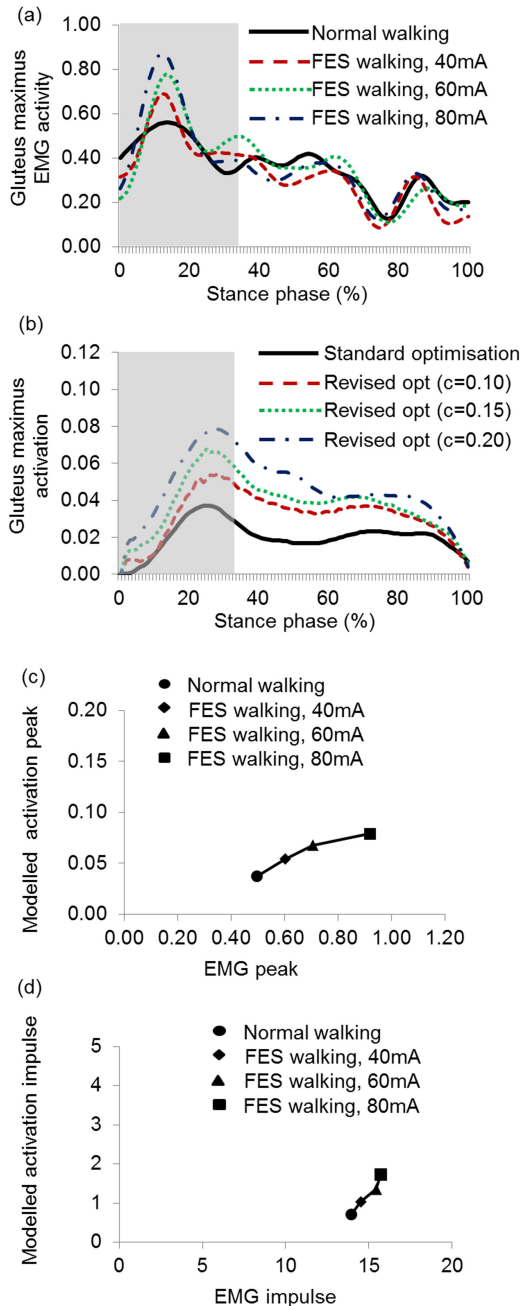
Fig. 3. (a) Measured EMG activity and (b) modelled activation from the optimisation (opt) model of GMAX for a representative subject (S1). Grey shaded areas indicate early stance phase. Measured EMG activity versus (c) modelled activation in GMAX early stance peak and (d) impulse for the same subject (S1). The other 12 subjects are shown in Supplemental Figs. (a) and (b).

instrumented implant validation for studies combined with FES; such as has been used to validate musculoskeletal modelling for the hip and knee [15], [35].

In this study BFLH was selected because of its clinical relevance: it has been used to generate hip extension for patients with paraplegia [6] and to improve knee stability for patients with ACL deficiencies [24]. There are other clinical conditions where muscle activation could be used therapeutically, for example, to correct foot drop following stroke through the stimulation

of tibialis anterior [5] or to attenuate muscle atrophy associated with total knee arthroplasty through the stimulation of vastus medialis [36]. The validation approach developed and tested here could potentially be used in these applications.

This study has some limitations. First, the test cohort comprised only healthy, able-bodied subjects. In order to study the clinical effect of FES on patients with neuromuscular disorders, kinematics and kinetics from patient groups are required as the movement strategies may be different from those of healthy subjects [37]. Patient-specific musculoskeletal modelling for these subjects would also enhance the modelling fidelity as some parameters in the model may need to be adjusted in order to represent the morphological changes due to the disorders, such as changes in muscle size and attachments [38].

In this study, muscle force during gait was quantified by minimising the sum of muscle activations cubed [27]. When compared with EMG measurement, this criterion has been shown to accurately predict muscle activation pattern during gait, cycling and other similar functional activities for healthy subjects [32], [39]. However, for patients with neuromuscular disorders, other physiological cost functions may be more representative of their movement strategies [40], [41]. Additionally, we recognize that EMG is not an absolute measure of muscle activation, and is appropriately used as a measure of change in activation [13].

The experiments in this study consistently measured first normal walking and then FES walking at increasing intensities. This approach was chosen to eliminate unwanted kinematics effects due to fatigue and discomfort. However, this may have introduced some bias and, therefore, for a systematic investigation of FES intervention during gait, the walking conditions could be randomized.

V. CONCLUSION

The study is the first to have validated the use of musculoskeletal modelling to quantify the effect of FES during gait in healthy subjects. The specific use, in this study, of FES for BFLH was shown to predictably increase GMAX activation. We propose using this approach to quantify the effect of FES on other muscles and activities.

ACKNOWLEDGMENT

REFERENCES

[1] E. F. Hodkin et al., "Automated FES for upper limb rehabilitation following stroke and spinal cord injury," IEEE Trans. Neural Syst. Rehabil. Eng., vol. 26, no. 5, pp. 1067–1074, May 2018.
[2] R. Kobetic et al., "Muscle selection and walking performance of multi-channel FES systems for ambulation in paraplegia," IEEE Trans. Rehabil. Eng., vol. 5, no. 1, pp. 23–29, Mar. 1997.
[3] N. Sharma et al., "Dynamic optimization of FES and orthosis-based walking using simple models," IEEE Trans. Neural Syst. Rehabil. Eng., vol. 22, no. 1, pp. 114–126, Oct. 2014.
[4] R. Kobetic and E. B. Marsolais, "Synthesis of paraplegic gait with multichannel functional neuromuscular stimulation," IEEE Trans. Rehabil. Eng., vol. 2, no. 2, pp. 66–79, Dec. 1994.

[5] G. M. Lyons *et al.*, "A review of portable FES-based neural orthoses for the correction of drop foot," *IEEE Trans. Neural Syst. Rehabil. Eng.*, vol. 10, no. 4, pp. 260–279, Dec. 2002.

[6] K. H. Ha *et al.*, "An approach for the cooperative control of FES with a powered exoskeleton during level walking for persons with paraplegia," *IEEE Trans. Neural Syst. Rehabil. Eng.*, vol. 24, no. 4, pp. 455–466, Apr. 2016.

[7] L. Rane and A. M. J. Bull, "Functional electrical stimulation of gluteus medius reduces the medial joint reaction force of the knee during level walking," *Arthritis Res. Therapy*, vol. 18, no. 1, p. 255, Nov. 2016.

[8] G. T. Yamaguchi and F. E. Zajac, "Restoring unassisted natural gait to paraplegics via functional neuromuscular stimulation: A computer simulation study," *IEEE Trans. Biomed. Eng.*, vol. 37, no. 9, pp. 886–902, Sep. 1990.

[9] C. F. Chen *et al.*, "Reducing anterior tibial translation by applying functional electrical stimulation in dynamic knee extension exercises: Quantitative results acquired via marker tracking," *Clin. Biomech.*, vol. 28, no. 5, pp. 549–554, Apr. 2013.

[10] N. L. Azmi *et al.*, "Activation of biceps femoris long head reduces tibiofemoral anterior shear force and tibial internal rotation torque in healthy subjects," *PLoS One.*, vol. 13, no. 1, Jan. 2018, Art. no. e0190672.

[11] A. Erdemir *et al.*, "Model-based estimation of muscle forces exerted during movements," *Clin. Biomech.*, vol. 22, no. 2, pp. 131–154, Feb. 2007.

[12] B. J. Fregly *et al.*, "Grand challenge competition to predict in vivo knee loads," *J. Orthopeadic Res.*, vol. 30, no. 4, pp. 503–513, Apr. 2012.

[13] M. E. Lund *et al.*, "On validation of multibody musculoskeletal models," *Proc. Inst. Mech. Eng. Part H, J. Eng. Med.*, vol. 226, no. 2, pp. 82–94, Feb. 2012.

[14] B. Kirking *et al.*, "A multiaxial force-sensing implantable tibial prosthesis," *J. Biomech.*, vol. 39, no. 9, pp. 1744–1751, 2006.

[15] D. D. D'Lima *et al.*, "An implantable telemetry device to measure intra-articular tibial forces," *J. Biomech.*, vol. 38, no. 2, pp. 299–304, Feb. 2005.

[16] B. C. Fleming and B. D. Beynnon, "In vivo measurement of ligament/tendon strains and forces: A review," *Ann. Biomed. Eng.*, vol. 32, no. 3, pp. 318–328, Mar. 2004.

[17] M. Giroux *et al.*, "EMG-based validation of musculo-skeletal models for gait analysis," *Comput. Methods Biomech. Biomed. Eng.*, vol. 16, no. 1, pp. 152–154, Aug. 2013.

[18] S. R. Hamner *et al.*, "Muscle contributions to propulsion and support during running," *J. Biomech.*, vol. 43, no. 14, pp. 2709–2716, Oct. 2010.

[19] S. Sennels *et al.*, "Functional neuromuscular stimulation controlled by surface electromyographic signals produced by volitional activation of the same muscle: Adaptive removal of the muscle response from the recorded EMG-signal," *IEEE Trans. Rehabil. Eng.*, vol. 5, no. 2, pp. 195–206, Jun. 1997.

[20] K. C. Megill *et al.*, "On the nature and elimination of stimulus artifact in nerve signals evoked and recorded using surface electrodes," *IEEE Trans. Biomed. Eng.*, vol. BME-29, no. 2, pp. 129–137, Feb. 1982.

[21] E. Park and S. G. Meek, "Adaptive filtering of the electromyographic signal for prosthetic control and force estimation," *IEEE Trans. Biomed. Eng.*, vol. 42, no. 10, pp. 1048–1052, Oct. 1995.

[22] C. Frigo *et al.*, "EMG signals detection and processing for on-line control of functional electrical stimulation," *J. Electromyography Kinesiol.*, vol. 10, no. 5, pp. 351–360, Oct. 2000.

[23] I. Jonkers *et al.*, "The complementary role of the plantarflexors, hamstrings and gluteus maximus in the control of stance limb stability during gait," *Gait Posture*, vol. 17, no. 3, pp. 264–272, Jun. 2003.

[24] K. Takahashr *et al.*, "Effects of neuromuscular electrical stimulation after anterior cruciate ligament reconstruction on quadriceps strength, function, and patient-oriented outcomes: A systematic review," *J. Orthopaedic Sport Phys. Therapy*, vol. 66, no. 3, pp. 231–237, 2012.

[25] H. J. Hermens *et al.*, "Development of recommendations for SEMG sensors and sensor placement procedures," *J. Electromyography Kinesiol.*, vol. 10, no. 5, pp. 361–374, Oct. 2000.

[26] E. M. Arnold *et al.*, "How muscle fiber lengths and velocities affect muscle force generation as humans walk and run at different speeds," *J. Exp. Biol.*, vol. 216, pp. 2150–2160, Jun. 2013.

[27] Z. Ding *et al.*, "In vivo knee contact force prediction using patient-specific musculoskeletal geometry in a segment-based computational model," *J. Biomech. Eng.*, vol. 138, no. 2, Feb. 2016, Art. no. 021018.

[28] D. J. Cleather and A. M. J. Bull, "The development of a musculoskeletal model of the lower limb: Introducing FreeBody," *Roy. Soc. Open Sci.*, vol. 2, no. 6, Jun. 2015, Art. no. 140449.

[29] R. Dumas *et al.*, "A 3D generic inverse dynamic method using wrench notation and quaternion algebra," *Comput. Methods Biomech. Biomed. Eng.*, vol. 7, no. 3, pp. 159–166, Apr. 2004.

[30] R. D. Crowninshield and R. A. Brand, "A physiologically based criterion of muscle force prediction in locomotion," *J. Biomech.*, vol. 14, no. 11, pp. 793–801, 1981.

[31] G. T. Yamaguchi, *Dynamic Modeling of Musculoskeletal Motion: A Vectorized Approach for Biomechanical Analysis in Three Dimensions*. New York, NY, USA: Springer, 2001.

[32] K. C. Yeh and K. C. Kwan, "A comparison of numerical integrating algorithms by trapezoidal, Lagrange, and spline approximation," *J. Pharmacokinetics Biopharmaceutics*, vol. 6, no. 1, pp. 79–98, 1978.

[33] B. I. Prilutsky and R. J. Gregor, "Analysis of muscle coordination strategies in cycling," *IEEE Trans. Rehabil. Eng.*, vol. 8, no. 3, pp. 362–370, Sep. 2000.

[34] S. R. Hamner and S. L. Delp, "Muscle contributions to fore-aft and vertical body mass center accelerations over a range of running speeds," *J. Biomech.*, vol. 46, no. 4, pp. 780–787, Dec. 2013.

[35] M. O. Heller *et al.*, "Musculo-skeletal loading conditions at the hip during walking and stair climbing," *J. Biomech.*, vol. 34, no. 7, pp. 883–893, Jul. 2001.

[36] K. Avramidis *et al.*, "Effectiveness of electric stimulation of the vastus medialis muscle in the rehabilitation of patients after total knee arthroplasty," *Arch. Phys. Med. Rehabil.*, vol. 84, no. 12, pp. 1850–1853, 2003.

[37] J. G. Hincapie *et al.*, "Selection of shoulder and elbow muscles for a C5 SCI neuroprosthesis," *IEEE Trans. Neural Syst. Rehabil. Eng.*, vol. 16, no. 3, pp. 255–263, Jun. 2008.

[38] B. Medsker *et al.*, "Muscular, skeletal, and neural adaptations following spinal cord injury," *J. Orthopaedic Sports Phys. Therapy*, vol. 32, no. 2, pp. 65–74, Feb. 2002.

[39] B. I. Prilutsky, "Coordination of two-and one-joint muscles: functional consequences and Implications for motor control," *Motor Control*, vol. 4, no. 1, pp. 1–44, Jan. 2000.

[40] J. Dul *et al.*, "Muscular synergism-II. A minimum-fatigue criterion for load sharing between synergistic muscles," *J. Biomech.*, vol. 17, no. 9, pp. 675–684, 1984.

[41] P. Gerus *et al.*, "Subject-specific knee joint geometry improves predictions of medial tibiofemoral contact forces," *J. Biomech.*, vol. 46, no. 16, pp. 2778–2786, Sep. 2013.